# Malaysian Journal of Analytical Sciences (MJAS)



Published by Malaysian Analytical Sciences Society

# STRUCTURAL AND OPTICAL PROPERTIES OF DYSPROSIUM AND EUROPIUM CO-DOPED WITH YTTRIUM ALUMINIUM GARNET NANOCRYSTALLINE POWDERS PREPARED BY COMBUSTION SYNTHESIS

(Sifat-sifat Struktural dan Optikal daripada Serbuk Nanokristal Dysprosium dan Europium Diko-dopkan dengan Yattrium Aluminium Garnet yang Disediakan Secara Sintesis Pembakaran)

Abd Rahman Tamuri\*, Nor Ezzaty Ahmad, Nurliyana Nabilah Ghazali, Rosli Husin

Physics Department, Faculty of Science, Universiti Teknologi Malaysia, 81310 Johor Bahru, Malaysia.

\*Corresponding author: rahmantamuri@utm.my

Received: 13 November 2019; Accepted: 3 September 2020; Published: xx October 2020

#### **Abstract**

This paper presents the study on synthesized yttrium aluminum garnet (YAG), europium-doped YAG (YAG: Eu), and europium and dysprosium co-doped YAG (YAG: Eu, Dy) phosphors prepared by combustion synthesis (CS) using a mixture of fuel (urea). The effects of Eu3+ and Dy3+ ions concentration and annealing temperature were analysed using by X-ray diffraction (XRD) and photoluminescence (PL). YAG nano-crystalline powders were calcined at a temperature range of 900 °C to 1200 °C for 4 hours. Europium and dysprosium were added in different concentrations in the range of 0.1 at.% to 1.0 at.% to the coarsened pure YAG particles to understand its influences on the optical properties and sintered microstructures. The doping of YAG: Eu and co-doped YAG: Eu, Dy was calcined at 1100 °C for 4 hours. X-ray diffraction results showed the phosphors are single-phase YAG with crystalline sizes ranging from 30 to 40 nm. The room temperature photoluminescence results confirmed the introduction of the ion in the host lattice and its optical activation for all the Eu3+ and Dy³+ ions concentrations. The CIE1931 color coordinates showed the sample's emission laid in the near red region for Eu³+ ion concentration and near white region for the addition of Eu³+ and Dy³+ ion concentration. Eu³+ ion concentration of 1.0 at.% achieved the highest emission spectra intensity while the highest emission spectra was achieved at 0.5 at.% for Dy³+ ion concentration and the ion luminescence were preferentially excited with 395 nm for YAG: Eu while, 353 nm for YAG: Eu, Dy wavelength photons.

Keywords: YAG: Eu, Dy, europium, dysprosium, combustion synthesis, emission, urea

#### Abstrak

Kertas kerja ini membentangkan kajian hasil sintesis yttrium aluminium garnet (YAG), YAG Europium-doped (YAG: Eu) dan europium dan dysprosium bersama-sama doped YAG (YAG: Eu, Dy) fosfor yang disediakan oleh sintesis pembakaran (CS) menggunakan campuran bahan api (urea). Kesan kepekatan Eu³+ dan Dy³+ ion dan suhu kalsinasi telah dikaji oleh belauan sinar-X (XRD) dan fotoluminesens (PL). Serbuk YAG nano-kristal telah dikalsinasi dalam julat suhu 900 °C hingga 1200 °C selama 4 jam. Europium dan dysprosium ditambah dengan kepekatan yang berlainan dalam julat 0.1% hingga 1.0% kepada zarah YAG tulen untuk memahami pengaruhnya terhadap sifat optikal dan mikrostruktur sintered. Dop YAG: Eu dan ko-dop YAG: Eu, Dy telah dikalsinasi pada suhu 1100 °C untuk 4 jam. Keputusan belauan sinar-X menunjukkan bahawa fosfor adalah berfasa tunggal

# Abd Rahman et al: STRUCTURAL AND OPTICAL PROPERTIES OF DYSPROSIUM AND EUROPIUM CO-DOPED WITH YTTRIUM ALUMINIUM GARNET NANOCRYSTALLINE POWDERS PREPARED BY COMBUSTION SYNTHESIS

YAG dengan saiz kristal antara 30 nm hingga 40 nm. Hasil fotoluminensi pada suhu bilik mengesahkan pengenalan ion dalam kekisi tuan rumah dan pengaktifan optikal untuk semua kepekatan Eu<sup>3+</sup> dan Dy<sup>3+</sup> ions. Koordinat warna CIE1931 menunjukkan bahawa spektrum pancaran sampel terletak di kawasan merah berhampiran untuk kepekatan Eu<sup>3+</sup> ion dan berhampiran kawasan putih untuk penambahan kepekatan Eu<sup>3+</sup> dan Dy<sup>3+</sup> ion. Keamatan spektrum pancaran tertinggi dicapai untuk kepekatan Eu<sup>3+</sup> ion pada 1.0 % sementara kepekatan 0.5% pada ion Dy<sup>3+</sup> dan pengujaan lebih sesuai pada panjang gelombang 395 nm untuk YAG: Eu manakala, 353 nm untuk YAG: Eu, Dy.

Kata kunci: YAG: Eu, Dy, europium, dysprosium, sintesis pembakaran, pancaran, urea

#### Introduction

Yttrium aluminum garnet, Y<sub>3</sub>Al<sub>5</sub>O<sub>12</sub> (YAG) materials have received huge interest in research for their wide range of applications found in fluorescent and solid-state lasers [1]. A conventional route has been introduced in obtaining YAG by combustion via self-propagating high temperature (SHS) for a fast and efficient productivity in various materials [2]. Good conductivity, high purity of products, reduced cost and increased materials size are some of the advantages that are contributed by SHS. Recently, attention has shifted to conventional light sources by using a white light-emitting diode (w-LED) for its high luminescent efficiency and energy-saving characteristics where the Dy3+ transition bands emit white light with small red emission [3]. Thus, the Eu<sup>3+</sup> acts as efficient activators that contribute to red emission when occupied with the host. Previously, the solid-state method and the use of high temperature was used to synthesize pure yttrium aluminum garnets. Heat treatment below 1600°C was required to distinguish between YAP and YAM phases [4]. Furthermore, other various conventional routes were used such as sol-gel, co-precipitation, hydrothermal synthesis, combustion synthesis [5-11].

The particle size and irregular morphology were produced with high temperatures that reduce its luminescent properties. Thus, by reducing particle sizes, it will increase the resolution of the material. The combustion synthesis also helps in good crystallinity and enhances the efficiency of luminescence with evading absorbed ligands. During the past decades, the novel and enhanced properties of nanostructured materials have attracted considerable attention because of their interesting chemical and physical properties. The nanostructure materials may have applications in

the development of a novel type of luminescent material for display applications. In particular, the Mn-doped ZnS nanocrystal can yield both high luminescent efficiencies and lifetime shortening [12-17]. This greatly promotes the development of rare-earth-doped nanophosphors. YAG: Eu<sup>3+</sup> is a red phosphor widely used in optical display and lighting applications. Furthermore, YAG: Eu<sup>3+</sup> can be used in fluorescence thermometry because its fluorescence properties vary with temperature [16].

Hence, the purpose of this paper is to report on the formation of YAG phosphors by low-temperature combustion synthesis and the influence of concentration in Eu<sup>3+</sup>and Dy<sup>3+</sup> doping ions on the YAG. In this work, europium doped YAG that exhibited orange-red emission was synthesized and the effect of Dy<sup>3+</sup> codoping on structural and luminescent properties will be studied. The results revealed that this technological approach enables us to achieve a stable single-phase structure of garnet and orange-red emission of YAG: Eu can be efficiently improved by incorporating a small amount of Dy<sup>3+</sup> ions.

### **Materials and Methods**

#### Study area

The starting material, Y<sub>2</sub>O<sub>3</sub>(99.99%), Al(NO<sub>3</sub>)<sub>3</sub>.9H2O, and CH<sub>4</sub>N<sub>2</sub>O (urea) used as a fuel by Sigma Aldrich and europium were added with a concentration between 0.1 to 1.0 mol%, while dysprosium, used as a co-dopant, was added with a concentration between 0.1 to 0.5 mol% using redox mixtures of strict stoichiometric amounts of metal oxides and urea, and initiates the combustion at 500 °C. The Y<sub>2</sub>O<sub>3</sub>, Eu<sub>2</sub>O<sub>3</sub>, Dy<sub>2</sub>O<sub>3</sub> powders were converted into the corresponding nitrate by dissolving in 2.5 M of nitric acid. 15 g of aluminum nitrate,

Al(NO<sub>3</sub>)<sub>3</sub>.9H<sub>2</sub>O, 9.6 g of urea, CH<sub>4</sub>N<sub>2</sub>O, Y(NO<sub>3</sub>)<sub>3</sub>.6H<sub>2</sub>O, Eu(NO<sub>3</sub>)<sub>3</sub>.6H<sub>2</sub>O, Dy(NO<sub>3</sub>)<sub>3</sub>.6H<sub>2</sub>O, and 30 mL distilled water were mixed using a magnetic stirrer for 30 minutes until a colorless aqueous solution was formed. The solution was transferred into a 200 mL alumina crucible and kept in a furnace that has been pre-heated at 500 °C. The removal of water took place before combustion initiated until it formed a voluminous fluffy mass and taken out immediately. The fluffy mass was cooled for 30 minutes at room temperature, then transferred into a mortar. The fine powder was obtained from grinding and sieving. 2 g for each sample powders were transferred into a 10 mL alumina crucible and kept at 1100 °C for 4 hours for the calcination process. The powders were taken out and left for the cooling process for 30 minutes before grinding the powders that were then weighed and kept in zipped packaging plastic bags.

The phase of the samples was determined by using X-ray Diffraction (XRD) and the photoluminescence measurement was recorded by a Horiba FluoroMax-4 Spectroflourometer of which offered extended performance with detection of emission spectra of up to 1700 nm. X-ray profile analysis is a simple and powerful tool to estimate the crystallite size and lattice strain [18]. Among the available methods to estimate the crystallite size and lattice strain are the pseudoVoigt functions, Rietveld refinement, and Warren-Averbach analysis [19-22]. Williamson-Hall (W-H) analysis is a simplified integral breadth method where both size-induced and strain-induced broadening are deconvoluted by considering the peak width as a function of  $2\theta$  [23].

The International Commission on Illumination (CIE) parameters such as color coordinates (x, y) were calculated to know the photometric characteristics of the prepared samples [24, 25]. The CIE coordinates were estimated using a PL emission spectrum. The value of CIE parameter of the phosphor is highly useful for the production of artificial white light which is similar to the natural white light owing to its better spectral overlap in white LEDs and solid-state display applications.

#### Results and Discussion

## X-ray analysis

Figure 1 represents the XRD diffraction patterns of YAG, YAG: Eu and YAG: Eu, Dy calcined at 1100 °C for 4 hours. It can be observed that all the diffraction peaks were matched well with the JCPDS No. 33-0040, the XRD maximum was observed at  $2\theta \sim 33.33^{\circ}$ . There is a slight shift in the diffraction pattern for YAG: Eu and YAG: Eu, Dy towards a high angle compared to pure YAG. The lattice parameter was calculated as YAG (12.0183 Å), YAG: Eu (11.976 Å), and YAG: Eu, Dy (12.0148 Å) using the combined formula of Bragg and the interplanar distance of the cubic structure. The lattice parameter of the europium doped YAG and dysprosium co-doped YAG was higher than the pure YAG crystal. The radius of Eu<sup>3+</sup> ion (0.950 Å) and Dy<sup>3+</sup> ion (0.908 Å) is higher than  $Y^{3+}$  ion (0.893 Å) ions. Factors that cause a decrease in lattice parameter are due to the contribution of the stress, strain, dislocation and defects or irradiation effects that alter the lattice parameter [24]. But, Eu<sup>3+</sup> and Dy<sup>3+</sup> ions are successfully substituted Y<sup>3+</sup> ion that contain small amounts of Eu<sup>3+</sup> and Dy<sup>3+</sup> ions that did not change the crystalline structure but broadened by increasing of the crystallite size. As the dopants were introduced to pure YAG phosphor, the size increased thus forming a diffraction pattern comparable to pure YAG.

To simplify the method of studying the changes of the strain and size the W-H plot and size strain plot method can be used. This is where the size-induced and straininduced broadening contributes to the peak as a function of  $2\theta$ . The peak width derived from crystallite size varies as  $1/\cos\theta$ , whereas the strain varies as  $\tan\theta$ . Figure 2 shows the W-H plots drawn with 4 sin  $\theta$  along the x-axis and  $\beta$  cos  $\theta$  along the y-axis for sample YAG pure, YAG:Eu and YAG:Eu,Dy. The value of the slope and the y-intercept of the fitted line represent the strain and the crystallite size of the samples as shown in Table 1. It was found that the crystallize size is bigger compared to the crystallite size calculated from Scherrer's equation. The strain was assumed to be uniform in all crystallographic directions, which takes consideration the isotropic nature of the crystal, where the material properties are independent of the direction

along which they are measured. The Scherrer's equation and W-H analysis were in agreement for this report.

#### Photoluminescence

Figure 3 presents the emission spectrum of the nanopowders YAG: Eu with 0.1, 0.5, 1.0 at.%. The spectrum consists of bands that belong to the characteristic emission of Eu<sup>3+</sup> bands that correspond to the transitions from the excited state <sup>5</sup>D<sub>0</sub> at 395 nm. The stark component of the  ${}^5D_0 \rightarrow {}^7F_1$  transition is observed at (590, 595 nm). The peaks corresponding to the  ${}^{5}D_{0} \rightarrow {}^{7}F_{4}$  (695, 709 nm),  ${}^{5}D_{0} \rightarrow {}^{7}F_{3}$  (649, 655 nm), and  $^5D_0 \rightarrow ^7F_2$  (609, 629 nm) transition are weaker. It is worth mentioning that all the above-listed transitions are the characteristics of a well in YAG: Eu that is in agreement with Kumar, M et al. [4]. According to the selection rules, magnetic dipole transition  ${}^5D_0 \rightarrow {}^7F_1$  is allowed while electric dipole transition  ${}^5D_0 \rightarrow {}^7F_2$  (609, 629 nm) is forbidden. Thus, the emission intensity of the transition  ${}^5D_0 \rightarrow {}^7F_1$  is higher than the transition  $^{5}D_{0} \rightarrow ^{7}F_{2}$ . intensity The spectral increased proportionally to the concentration of Eu<sup>3+</sup>.

Figure 4 shows the luminescence spectra and transition energy levels of YAG:Eu phosphors co-doped with Dy<sup>3+</sup> ions ranging from 450 nm to 680 nm and excitation

wavelength of 353 nm. The prominent emission peaks were observed at blue emission (483 nm) and yellow emission (582 nm) [4]. The transition corresponded to  $^{4}D_{9/2} \rightarrow ^{6}H_{15/2}$  $(483 \text{ nm}), {}^{4}D_{9/2} \rightarrow {}^{6}H_{15/2}$ (582 nm),  $^{4}D_{9/2} \rightarrow ^{7}F_{1}$  (589 nm) and  $^{4}D_{9/2} \rightarrow ^{7}F_{2}$  (608 and 629 nm). Six emission bands were observed from the results such as 596 nm, 610 nm, 630 nm, 649 nm and 710 nm which corresponds to the emission bands and transition of Eu<sup>3+</sup> in Figure 3(a). Due to the strong influence of the environment, Dy3+ ions contributed to the blue and yellow emission while Eu<sup>3+</sup> enhanced the red emission of the phosphors. The spectral intensity of 1.0 mol at % Dy<sup>3+</sup> is the highest compared to 0.5 and 0.1 mol at.% thus, these characteristics satisfy the requirement for YAG phosphors for white light-emitting diode (w-LED) applications.

The chromaticity coordinates for ideal white light is located at  $(0.313,\ 0.329)$  [9]. Figure 5(a) shows the Commission International de I'Echairage (CIE)1931 chromaticity coordinates for the YAG:Eu, yDy (y = 0.1, 0.3 and 0.5 mol%) phosphors excited at 353 nm and Figure 5(b) the colour coordinates of 0.1 at.% YAG:Eu,Dy phosphor (x,y) =  $(0.310,\ 0.353)$  are close to the ideal white emission colour. This result satisfies the requirement for YAG phosphors for white lightemitting diode (w-LED) applications.

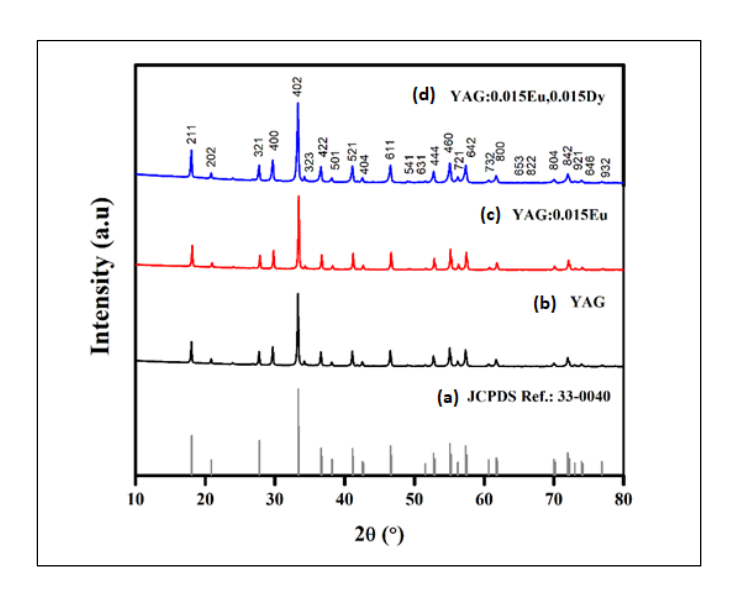


Figure 1. XRD pattern of selected (a) JCPDS Ref.:33-0040, (b) YAG pure, (c) YAG:0.015Eu and (d) YAG:0.015Eu, 0.015Dy. As dopants are introduced, pattern is comparable to pure YAG

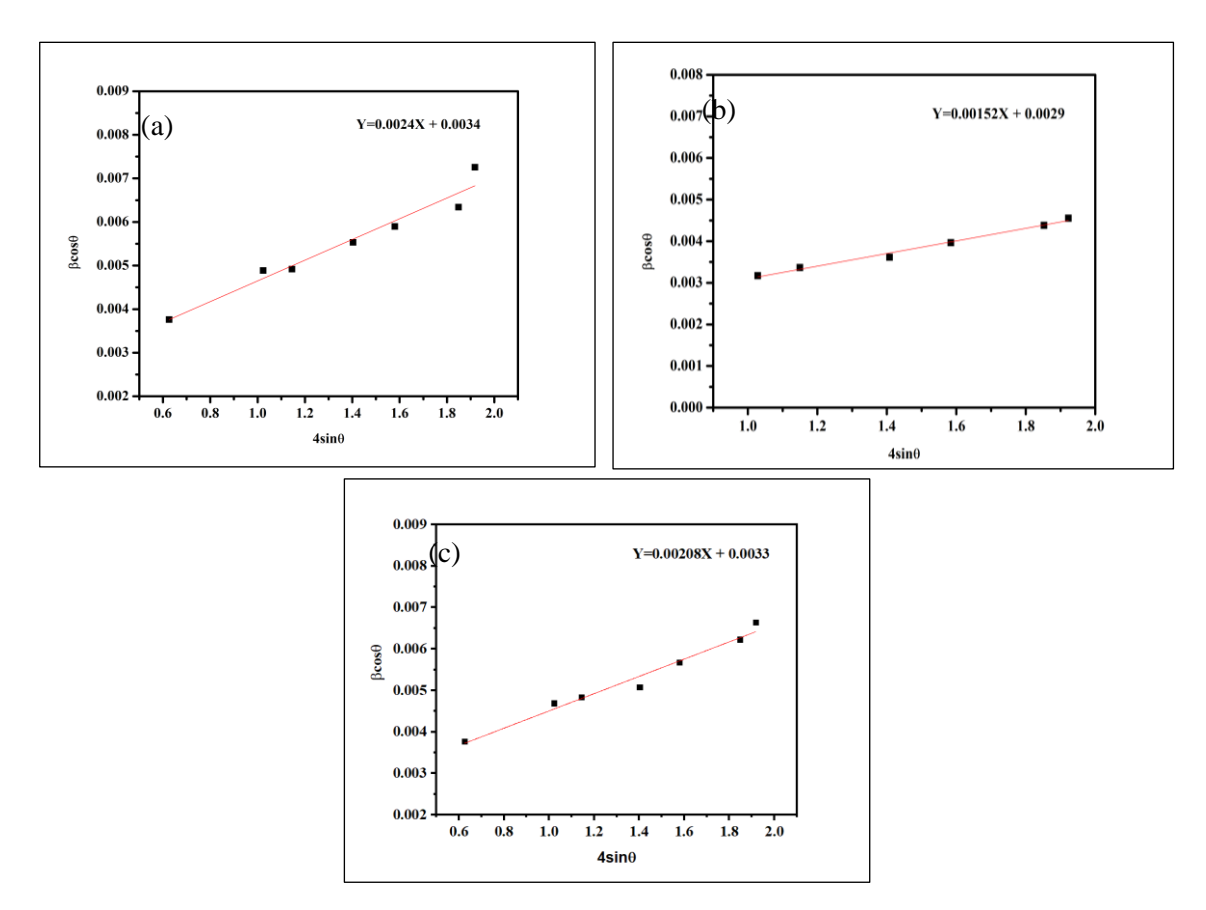


Figure 2. The Williamson Hall plot (a) YAG phosphors, (b) 0.5 mol % for YAG: Eu (c) 0.5 mol% for YAG: Eu, Dy

Table 1. Crystallite size of YAG, YAG: Eu and YAG: Eu, Dy

Crystallite size* (nm) (Scherrer's method)	Compound	Crystallite size* (nm) (W-H method)	Microstrain ε
38	YAG	40.3	2.40
40	YAG:0.015Eu	47.3	1.52
30	YAG:0.015Eu,0.015Dy	41.5	2.08

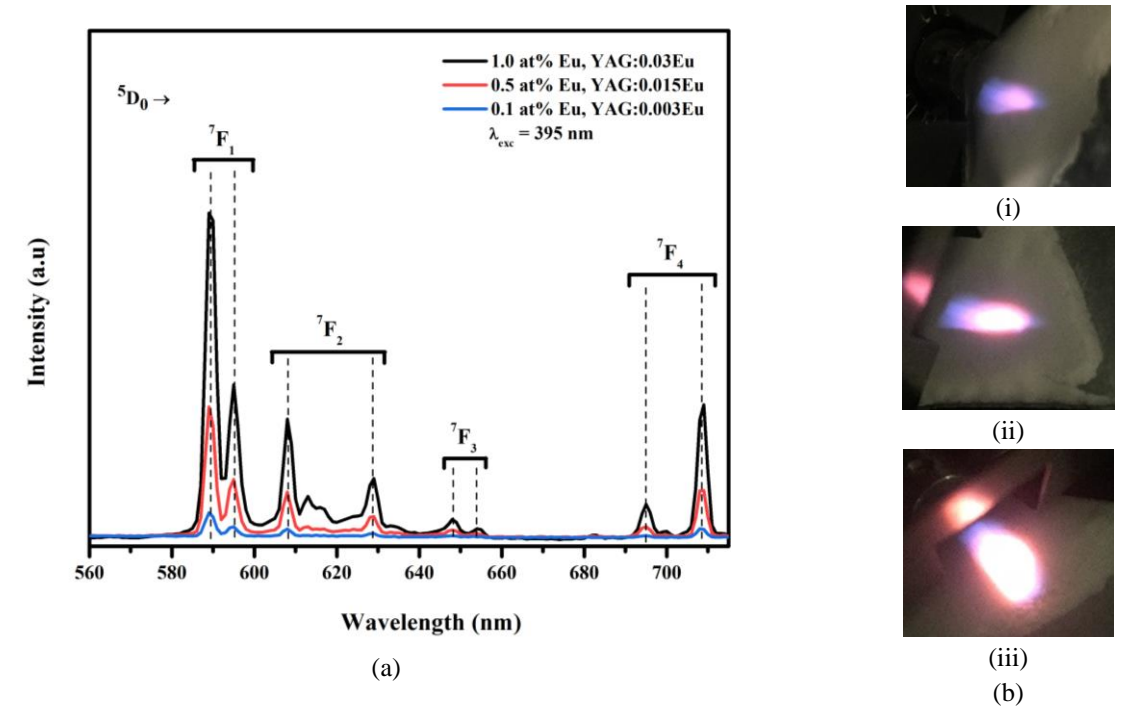


Figure 3. (a) The PL emission spectra of samples YAG:Eu with 0.1,0.5,1.0 mol % concentration excited at 395 nm. (b) The colour emitted by the YAG:Eu sample of (i) 0.1 %, (ii) 0.5 % and (iii) 1.0 % respectively

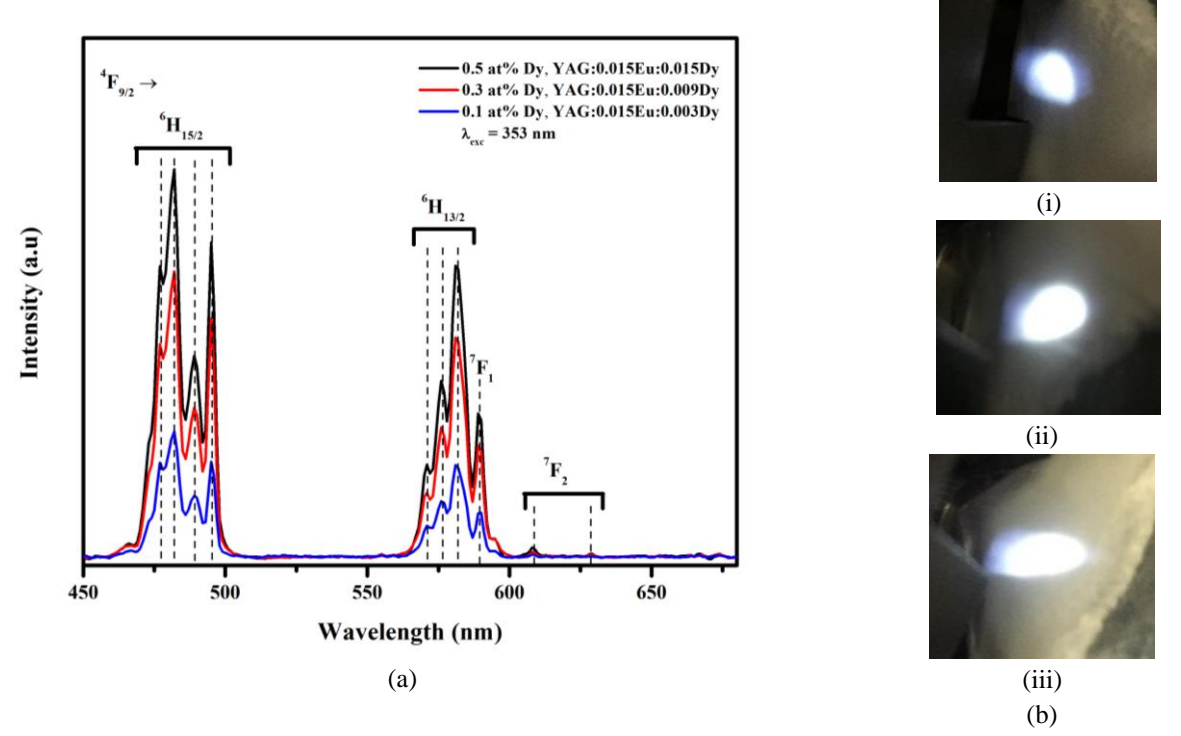
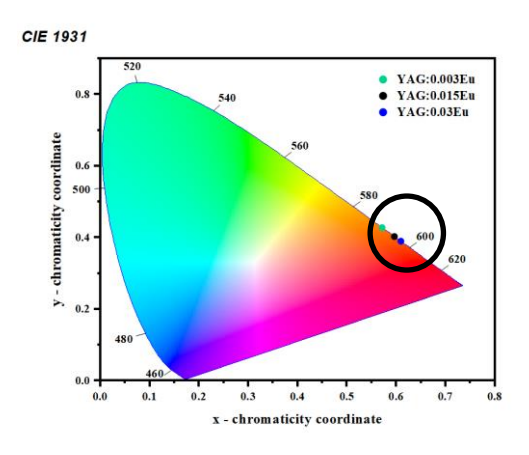


Figure 4. (a) YAG:Eu,Dy with 0.5 mol % of europium and 0.1, 0.3, 0.5% concentration of dysprosium, excited at 353 nm. (b) The colour emitted by the YAG:Eu,Dy sample of (i) 0.1 %, (ii) 0.3 %, and (iii) 0.5 % respectively



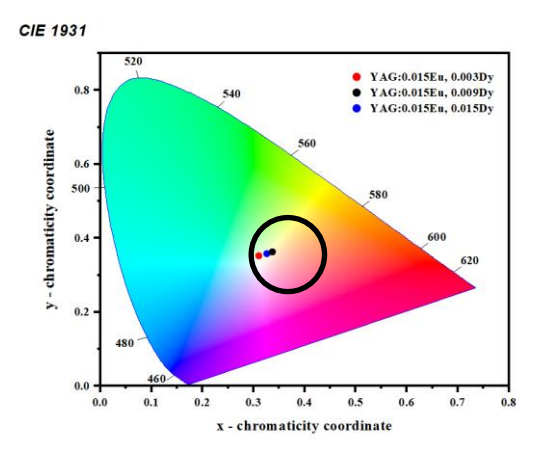


Figure 5. The CIE coordinates of (a) YAG: Eu with 0.1, 0.5, 1.0 mol% concentration excited at 395 nm (b) YAG: Eu, Dy with 0.5 mol% of europium and 0.1, 0.3, 0.5% concentration of dysprosium, excited at 353 nm

#### Conclusion

The pure YAG and doped YAG: Eu and YAG: Eu, Dy with different concentrations have been successfully synthesised by using the combustion synthesis method. The sample size of 40nm was confirmed using Scherrer's method and W-H method. The Eu<sup>3+</sup> emitted red light, thus proving the fact that Eu<sup>3+</sup> ions show promising red light emission. However, a combination of Eu<sup>3+</sup> and Dy<sup>3+</sup> in YAG gave white emission. From the chromaticity diagram of YAG: Eu, 1.0 mol% of Eu<sup>3+</sup> ions were located at the reddest region (0.60916, 0.39032) while for Dy<sup>3+</sup> ions, 0.1, 0.3, and 0.5 mol% concentrations were used. The emission spectra and transition energy were observed within the range of 450 nm and 680 nm. The excitation wavelength was set to 353 nm. Moreover, the chromaticity shows that 0.1 mol% of Dy<sup>3+</sup> ions were nearest to the ideal white light value which is (0.31002, 0.35291).

#### Acknowledgment

The authors gratefully acknowledge the Ministry of Education (MOE) of Malaysia and Universiti Teknologi Malaysia for providing financial support under Grant No. Q.J1300000.2526.10H20. We would also like to extend our gratitude to the Faculty of Science, Universiti Teknologi Malaysia for providing experimental facilities for this research.

#### References

- Pan, Y. X., Wang, W., Liu, G. K., Skanthakumar, S., Rosenberg, R. A., Guo, X. Z. and Li, K. K. (2009). Correlation between structure variation and luminescence redshift in YAG:Ce. *Journal of Alloys and Compounds*, 488(2): 638-642.
- Jiang, J., Wang, P., He, W., Chen, W., Zhuang, H., Cheng, Y. and Yan, D. (2004). Self-propagating high-temperature synthesis of α-SiAlON doped by RE (RE=Eu,Pr,Ce) and codoped by RE and Yttrium. *Journal of American Ceramic Society*, 87(4): 703-705.
- Chong, J. Y., Zhang, Y., Wagner, B. K. and Kang, Z. (2013). Co-precipitation synthesis of YAG:Dy nanophosphor and its thermometric properties. *Journal of Alloys and Compounds*, 581: 484-487.
- Kumar, K. S., Lou, C., Xie, Y., Hu, L., Gowri, A.M., Xiao, D., Ye, H., Tang, L., and Didier, P. (2017). Energy transfer in co- and tri- doped Y<sub>3</sub>Al<sub>5</sub>O<sub>12</sub> phosphors. *Journal of Rare Earths*, 35(8): 775-782.
- Mithlesh, K., Mohapatra, M., and Natarajan, V. (2014). Luminescence characteristics of blue emitting ZnAl<sub>2</sub>O<sub>4</sub>:Ce nanophosphors. *Journal of Luminescence*, 149: 118-124.

# Abd Rahman et al: STRUCTURAL AND OPTICAL PROPERTIES OF DYSPROSIUM AND EUROPIUM CO-DOPED WITH YTTRIUM ALUMINIUM GARNET NANOCRYSTALLINE POWDERS PREPARED BY COMBUSTION SYNTHESIS

- Kurrey, M. S., Tiwari, A., Khokhar, M. S. K., Kher, R. S. and Dhoble, S.J. (2015). Thermoluminescence investigations of sol–gel derived and -irradiated rare earth (Eu and Nd) doped YAG nanophosphors. *Journal of Luminescence*, 164: 94-98.
- 7. Ya-Wei, L. and Su-Hsen, W. (2018). Fabrication and performance assessment of coprecipitation-based YAG:Ce nanopowders for white LEDs. *Microelectronic Engineering*, 199: 24-30.
- 8. Hora, D. A., Andrade, A. B., Ferreira, N. S., Teixeira, V. C., and dos S. Rezende, M.V. (2016). X-ray excited optical luminescence of Eu-doped YAG nanophosphors produced via glucose sol–gel route. *Ceramics International*, 42: 10516-10519.
- 9. Raju, G. S. R., Park, J. Y., Jung, H. C., Hyun, K, Y., Byung, K. M., Jung, H. J., and Jung, H. K. (2009). Synthesis and luminescent properties of low concentration Dy<sup>3+</sup>:GAP nanophosphors. *Optical Materials*, 31: 1210-1214.
- Kolesnikov, I. E., Tolstikova, D. V., Kurochkin, A. V., Manshina, A. A. and Mikhailov, M. D. (2014). Eu<sup>3+</sup> concentration effect on luminescence properties of YAG:Eu<sup>3+</sup> nanoparticles. *Optical Materials*, 37: 306-310.
- Guodong, X., Shengming, Z., Junji, Z., Sumei, W., Yanmei, L. and Jun, X. (2015). Sol–gel combustion synthesis and luminescent properties of nanocrystalline YAG:Eu<sup>3+</sup> phosphors. *Journal of Crystal Growth*, 283: 257-262.
- Bhargava, R. N., Gallagher, D., Hong, X. and Nurmikko, A. (1994). Optical properties of manganese-doped nanocrystals of ZnS. *Physics Review Letters*, 72(3): 416-419.
- 13. Zhang, W. P., Xi, P. B., Duan, C. K., Yan, K., Yi, M., Lou, L. R., Xia, S. D. and Krupa, J. C. (1998). Preparation and size effect on concentration quenching of nanocrystalline Y<sub>2</sub>SiO<sub>5</sub>: Eu. *Chemistry Physics Letters*, 292(1-2):133-136.
- 14. Allison, S. W. and Gillie, G. T. (1997). Remote thermometry with thermographic phosphors. *Review of Scientific Instruments*, 68(7): 2615-2650.
- 15. Mu, Z., Hu, Y., Wang, Yi., Wu, H., Fu, C., and Kang, F. (2011). Effect of substitution of Dy<sup>3+</sup> on structure and luminescence properties of Y<sub>3</sub>Al<sub>5</sub>O<sub>12</sub>:Ce<sup>3+</sup>. *Acta Optica Sinica*, 31(2): 0216007.

- 16. Lojpur, V., Egelja, A., Pantić, J., Dordević, V., Matović, B. and Dramićanin, M. D. (2014). Y<sub>3</sub>Al<sub>5</sub>O<sub>12</sub>:Re<sup>3+</sup> (Re=Ce, Eu, and Sm) nanocrystalline powders prepared by modified glycine combustion method. *Science of Sintering*, 46(1): 75-82.
- 17. Mote, V. D., Purushotham, Y. and Dole, B. N. (2012). Williamson-Hall analysis in estimation of lattice strain in nanometer-sized ZnO particles. *Journal of Theoretical and Applied Physics*, 6(6):1-8.
- Cullity, B. D., and Stock, S. R. (2001). Elements of X-ray diffraction, 3rd edition. Prentice Hall Publication, India.
- 19. Rietveld, H. M. (1967). Line profiles of neutron powder-diffraction peaks for structure refinement. *Acta Crystallographica*, 22(1): 151-152.
- Balzar, D. and Ledbetter, H. (1993). Voigt-function modeling in Fourier analysis of size- and strainbroadened X-ray diffraction peaks. *Journal of Applied Crystallography*, 26: 97-103.
- 21. Warren, B. E. and Averbach, B. L. (1950). The effect of cold-work distortion on X-ray patterns. *Journal of Applied Physics*, 21(6): 595-599.
- 22. Suryanarayana, C. and Grant Norton, M. (1998). X-ray diffraction: A practical approach. Springer, New York.
- 23. Anitha, S. N., and Jayakumari, I. (2015). Synthesis and analysis of nanocrystalline Fe<sub>2</sub>Mn<sub>2</sub>Ni<sub>0.5</sub>Zn<sub>1.5</sub>O<sub>9</sub> at different treating temperatures. *Journal of Nanoscience and Technology*, 1(1): 26-31.
- 24. Chowdhury, M. and Sharma, S. K. (2015). Spectroscopic behavior of Eu<sup>3+</sup> in SnO<sub>2</sub> for tunable red emission in solid state lighting devices. *RSC Advances*, 5: 51102-51109.
- 25. Ashwini, K. R., Premkumar, H. B., Darshan, G. P., Nagabhushana, H., Sharma, S., Prashantha, S. and Nagaswarupag, H. P. (2017). Synthesis and photometric properties of SrAl<sub>2</sub>O<sub>4</sub>: Gd<sup>3+</sup> nanophosphors via solution combustion method. *Materials Today: Proceedings*, 4: 12168-12173.